ELSEVIER

Thermochimica Acta 274 (1996) 231–242

thermochimica acta

Mixtures of *d*- and *l*-carvone: I. Differential scanning calorimetry and solid–liquid phase diagram

H.E. Gallis *, F. Bougrioua, H.A.J. Oonk, P.J. van Ekeren, J.C. van Miltenburg

Debye Institute, Department of Interfaces and Thermodynamics, Utrecht University, Padualaan 8, 3584 CH Utrecht, The Netherlands

Received 7 February 1995; accepted 9 August 1995

Abstract

Pure *l*-carvone and mixtures of *d*- and *l*-carvone have been studied by differential scanning calorimetry. The obtained curves of heat flow against temperature show the glass transition of the samples, followed by two crystallisation events and, finally, the melting of the carvone mixtures. The measured temperature of melting of pure *l*-carvone is (247.7 ± 0.5) K and the heat of fusion (11.55 ± 0.05) kJ mol^{-1}. Five precrystallised samples with compositions ranging from equal amounts of *d*- and *l*-carvone up to pure *l*-carvone have been studied. The carvone system shows mixed crystals at all compositions corresponding to a phase diagram with a minimum at equimolar composition. The data obtained by computer calculations agree with the experimental values, thus showing the thermodynamic consistency of the obtained phase diagram.

Keywords: Carvone; DSC; Mixed crystals; Phase diagram

---

1. Introduction

Within REALM (Réseau Européen sur les Alliages Moléculaires), a co-operation of French, Spanish and Dutch Universities, research is performed on molecular mixed crystals. This research has been extended with measurements on optical antipode systems. The thermodynamic and crystallographic properties of enantiomers are interesting from a scientific point of view and are of great importance in biomedical applications as a large amount of medicines consists of optically active compounds.

---

* Corresponding author. Tel.: 31 302 533211; Fax: 31 302 533946; E-mail: gallish@chem.ruu.nl.

SSDI 0040-6031(95)02716-5

The thermodynamic properties of a few candidate systems are investigated by differential scanning and adiabatic calorimetry.

Most pairs of optical antipodes form a so-called racemic compound containing equal amounts of *d*- and *l*-molecules. Conglomerates are formed in relatively few cases. The formation of mixed crystals of enantiomers is a rather uncommon phenomenon [1]. The desire to predict the formation of mixed crystals requires information on the systems showing spontaneous mixing. To this end, Kitaigorodskii [2], Chion et al. [3] and Haget [4], among others, tried to correlate pure component properties to thermodynamic mixing properties. The conditions for the occurrence of spontaneous mixing proved to be related to molecular homeomorphism, crystal cell isomorphism, and the presence of hydrogen bonding networks. More studies need to be conducted to ascertain the effect of these conditions which may be used to predict accurately the occurrence of the formation of mixed crystals.

The optical antipode system investigated in our research is the carvone system since it satisfies the conditions for the formation of mixed crystals. The composition of the mixtures is described by $(1-x)$ mole of *l*-carvone and x mole of *d*-carvone. Differential scanning calorimetry (DSC) was used to investigate the thermal behaviour of carvone mixtures during heating. The phase diagram of the carvone system was deduced from the thermal behaviour of five mixtures. Complementary data on the system are currently being obtained by adiabatic calorimetry.

2. Experimental

2.1. Materials and apparatus

d- and *l*-carvone, liquid at room temperature, were obtained from E. Merck Nederland B.V. Both products contained over 99% carvone but had different optical cleanness. The rotation measured on neat samples was $[\alpha]_D^{20} = +56.0^\circ$ and $[\alpha]_D^{20} = -58.8^\circ$ for *d*- and *l*-carvone respectively. The reported compositions were corrected assuming that the *d*-carvone as obtained was slightly contaminated with *l*-carvone.

All measurements were performed on a DSC 120 from Seiko Instruments Inc. using a heating rate of 2.5 K $\min^{-1}$. The DSC apparatus was calibrated with adamantane and water.

2.2. Methods

The temperature ranges for optimal nucleation and crystallisation of carvone are separated. The carvone mixtures were supercooled below the glass transition temperature. Crystallisation occurred during the heating of the samples.

The melting peaks of five mixtures were used to determine the solidus and liquidus, using auxiliary lines as described by Höhne et al. [5]. A solidus point corresponds to the extrapolated peak onset temperature (T_e). At this temperature the auxiliary line through the ascending peak slope intersects the linearly extrapolated initial base line, see Fig. 1a.

The determination of the liquidus points requires a correction for the shift of the peak temperature due to the heating of the sample, using the correct angle γ. The angle is obtained from a melting experiment using a pure component at the respective heating rate, see Fig. 1a, the slope of the drawn line being $\Delta\Phi/\Delta T_p = \tan\gamma$. For a pure component, the extrapolated peak onset temperature and the corrected peak temperature coincide. When examining a complex thermal event, the liquidus temperature can be found by drawing an auxiliary line at the angle γ to the interpolated base line, see Fig. 1b. The auxiliary line is drawn through that point of the DSC curve where the heat flow falls off exponentially.

3. Results

The thermal behaviour of pure *l*-carvone is shown in Fig. 2. The first DSC curve (denoted A) was measured on a sample which was supercooled below the glass

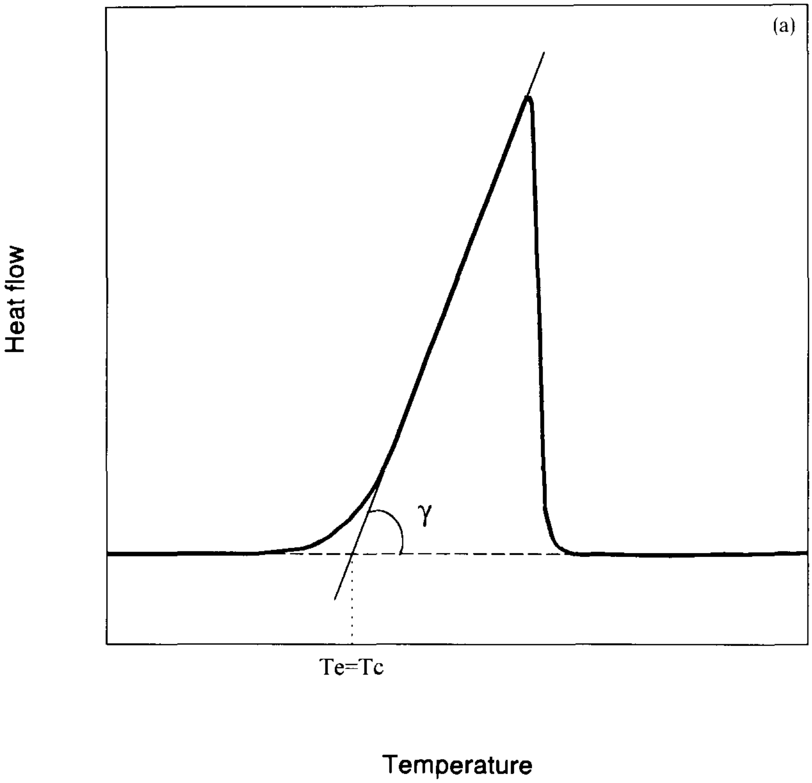

Fig. 1. (a) DSC curve of a pure component. The auxiliary line through the ascending peak slope intersects the extrapolated base line at T_e. (b) DSC curve of a complex thermal event. Auxiliary lines at the angle γ to the interpolated base line give the corrected peak maxima.

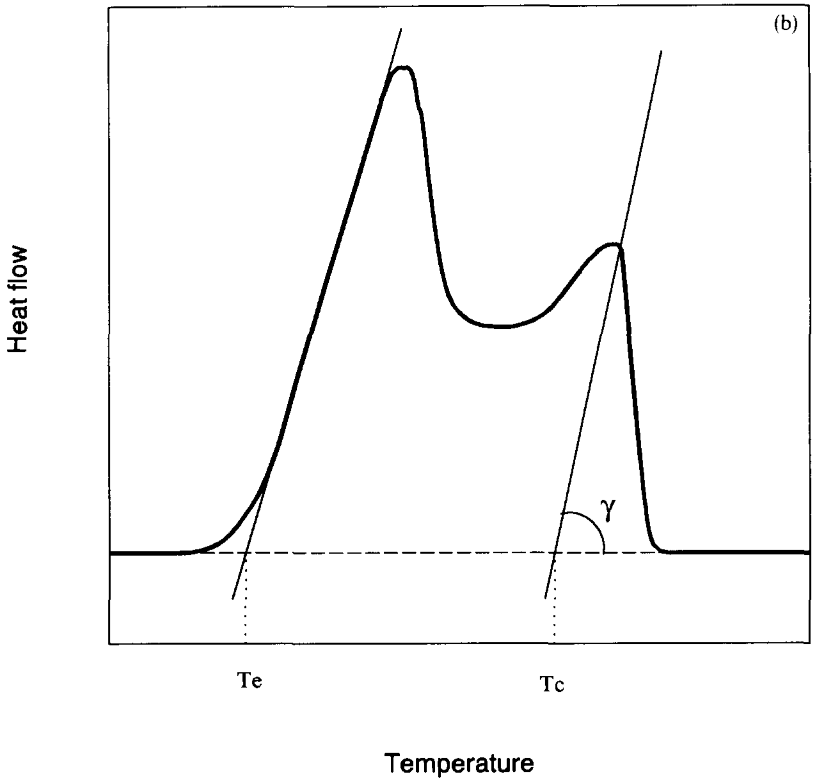

Fig. 1. (*Continued*)

transition temperature. The curve shows the glass transition at 171 K; next it shows a large crystallisation peak, followed by a small exothermic event that corresponds to a recrystallisation, and finally, the melting of the sample. The measured temperature of melting was $T^* = 247.7 \pm 0.5$ K and the heat of melting $\Delta_{\rm sol}^{\rm liq} H^* = 11.55 \pm 0.05$ kJ mol^{-1}. The second curve in Fig. 2 (denoted B) shows the melting peak of a precrystallised sample. The positions of the base line of the crystal phase and the liquid phase were independent of the thermal history. Moreover, position and size of the melting peak were not changed by the precrystallisation.

Heating supercooled mixtures of *d*- and *l*-carvone revealed a glass transition around 171 K, followed by one or two exothermic events and an endothermic event. Samples with compositions $0.5 \leqslant x \leqslant 0.75$ started to melt before the base line was reached. Consequently, it was not clear from this curve whether the crystallisation was complete. Moreover, the temperature and heat of melting could not be determined accurately using this DSC curve. See, for example, curve A in Fig. 3, which shows the DSC curve for a quickly cooled sample with composition $x = 0.66$.

In order to avoid this inconvenience, the supercooled carvone mixture was heated in a first measurement until the formed crystal started to melt. Then this partially

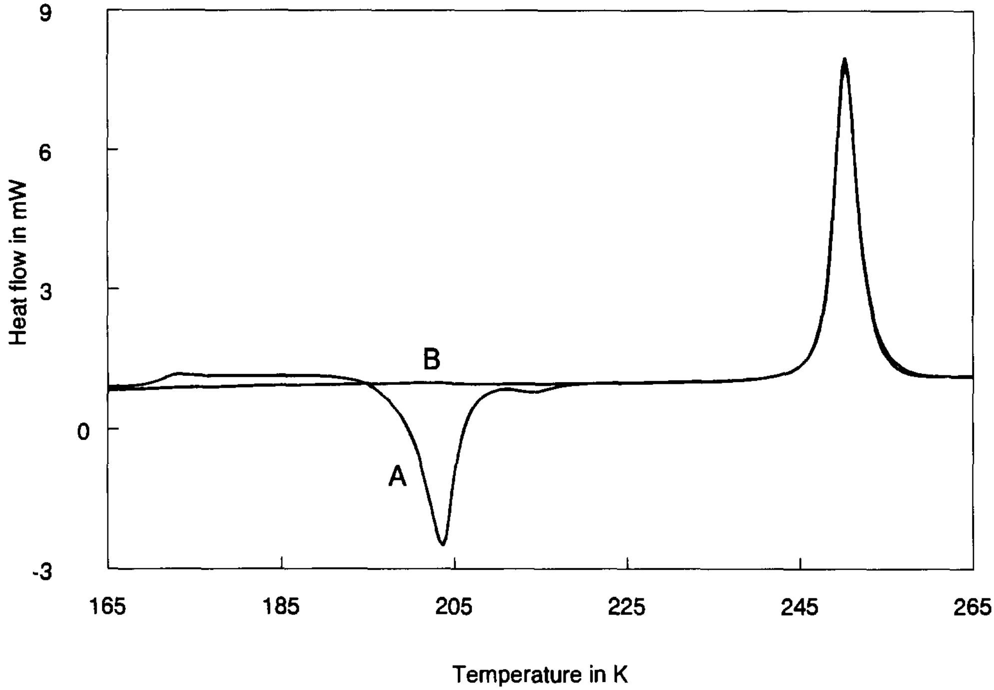

Fig. 2. DSC curve of pure *l*-carvone. Curve A was measured on a supercooled sample; curve B shows the melting peak of a precrystallised sample.

crystallised sample was cooled again, resulting in a completely crystallised sample. Then a second measurement was started. The precrystallised samples showed no exothermic effect, which indicates that all carvone was crystallised and recrystallised before the second measurement started. The transition temperatures and the heats of fusion were determined using five precrystallised samples with composition ranging from $x = 0.5$ to $x = 1$.

The results of these measurements are summarised in Table 1 and Fig. 4. The extrapolated peak onset corresponds to a solidus point and was determined using an auxiliary line through the ascending peak slope as described above. The shift of the peak maximum was calculated using an auxiliary line at an angle γ as described above and taking into account the different scaling of the axes.

The correct angle γ was determined using pure *l*-carvone in the following way

$$\tan\gamma = \Delta\Phi/\Delta T_p = 6.7/3.4 = 1.97.$$

This resulted in a shift of the peak maximum for $x = 0.66$, for example, of

$$\Delta T_p = \Delta\Phi/\tan\gamma = 8.7/1.97 = 4.4\ K$$

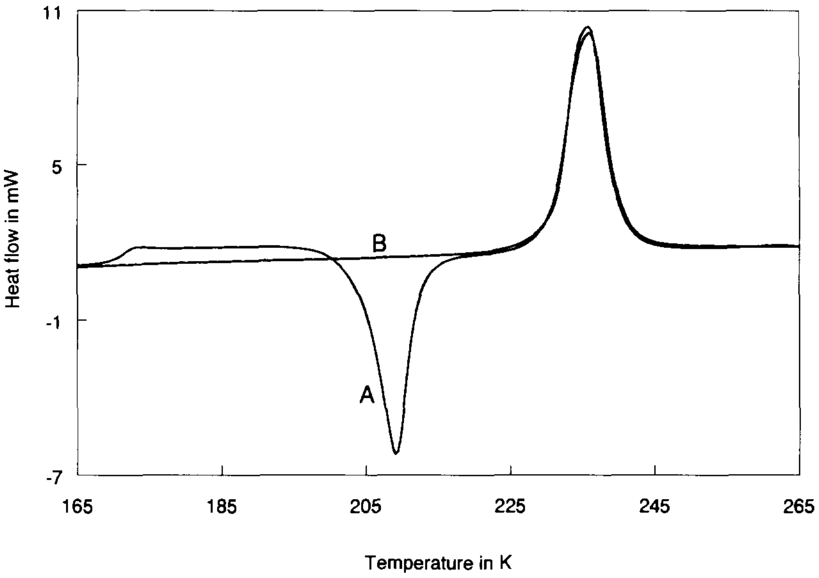

Fig. 3. DSC curve of a mixture with composition $x = 0.66$. Curve A was measured on a supercooled sample; curve B shows the melting peak of a precrystallised sample.

Table 1
DSC data for mixtures of *d*- and *l*-carvone

Composition x	Extrapolated peak onset T_e/K	Peak maximum T_p/K	Peak height $\Delta\Phi$/mW	Corrected peak max. T_c/K	Heat of fusion $\Delta_{sol}^{liq}H$/J mol^{-1}
0.5350	230.5	236.2	10.2	231.0	9449
0.6603	231.1	237.6	8.7	233.2	9239
0.7562	233.6	243.2	8.9	238.7	9689
0.8542	237.6	246.0	6.0	242.9	10230
1.0000	247.7	251.1	6.7	247.7	11552

Therefore the corrected peak maximum, corresponding to a liquidus point, for $x = 0.66$, became

$$T_c = T_p - \Delta T_p = 237.6 - 4.4 = 233.2\ K$$

The extrapolated peak onset and the corrected peak maximum both decline with decreasing x from $x = 1$ down to and including $x = 0.5$. The value of $\Delta_{sol}^{liq}H$ appears to decline with decreasing x from $x = 1$ down to and including $x = 0.66$. But several samples with an almost equimolar composition had a reproducible higher value for the heat of fusion than the sample with $x = 0.66$, see Table 1 and Fig. 5. However, from the

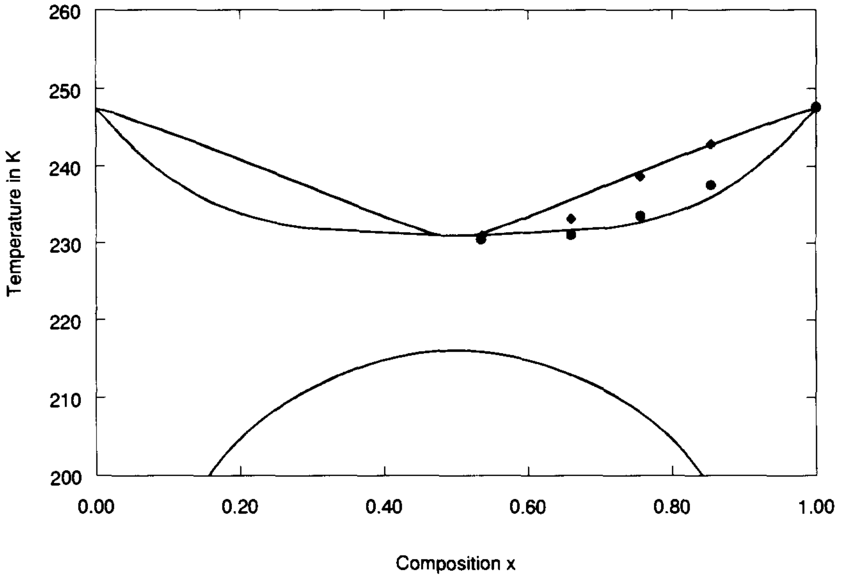

Fig. 4. Phase diagram of carvone: ●, experimental solidus points; ◆, experimental liquidus points; solid line, calculated phase diagram using Prophase.

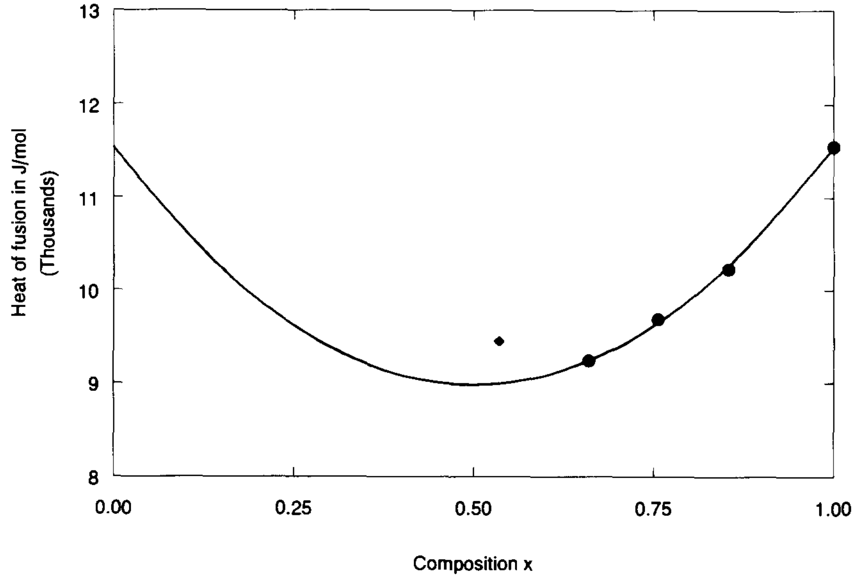

Fig. 5. ●, ◆; Measured heats of fusion against temperature. Solid line is the parabola through the measured heats of fusion of samples with a composition of $0.66 \leqslant x \leqslant 1.00$.

experimentally determined solidus and liquidus points as presented in Fig. 4, a smooth curve for the heat of fusion versus composition is expected.

A parabola was fitted through the measured heats of fusion for samples with a composition of $0.66 \leqslant x \leqslant 1.00$ and is presented in Fig. 5. The parabola can be described by

$$\Delta_{\text{sol}}^{\text{liq}} H(x) = \{11541 - 10233(1-x)\} \text{J mol}^{-1} \tag{1}$$

which is used in the discussion below.

The value for the heat of fusion of the equimolar mixtures was not reproducible with DSC measurements as it was dependent on thermal history. Hence, equimolar mixtures of *d*- and *l*-carvone will be investigated using adiabatic calorimetry.

4. Discussion

4.1. The phase diagram of the carvone system

Binary mixtures of enantiomers show three fundamental types of phase diagram as characterised by Bakhuis Roozeboom [6], corresponding to: (a) conglomerates, (b) racemic compounds and (c) mixed crystals, see Fig. 6. The mixed crystals that can be formed are: ideally mixed crystals (type I), mixed crystals corresponding to a phase diagram with a maximum (type II), and mixed crystals corresponding to a phase diagram with a minimum (type III).

In order to determine which type of phase diagram would be the most likely for the carvone system, the following conclusions were drawn from the DSC measurements. The experimentally determined onset and maximum of the melting peak versus composition are presented in Fig. 4. This figure clearly shows that the carvone system forms mixed crystals corresponding to a phase diagram with a minimum. This interpretation was supported by the observation that the beginning of the melting peak (T_e) changed with composition. Consequently, a phase diagram of the eutectic type, which is type (a) or (b), is not probable. Hence, the DSC measurements on mixtures of *d*- and *l*-carvone indicated that mixed crystals are formed at all compositions.

The thermal behaviour of a sample with equal amounts of *d*- and *l*-carvone is currently being studied using adiabatic calorimetry. Measurements under adiabatic conditions might disclose why the value of the heat of fusion of the equimolar samples as measured with a DSC apparatus was dependent on thermal history and higher than what would be expected from the determined phase diagram.

4.2. Prophase calculations

The computer program Prophase [7] was used to check the thermodynamic consistency of the proposed phase diagram. The computer program calculates the mole fractions of the coexisting phases for a specified set of temperatures using the tempera-

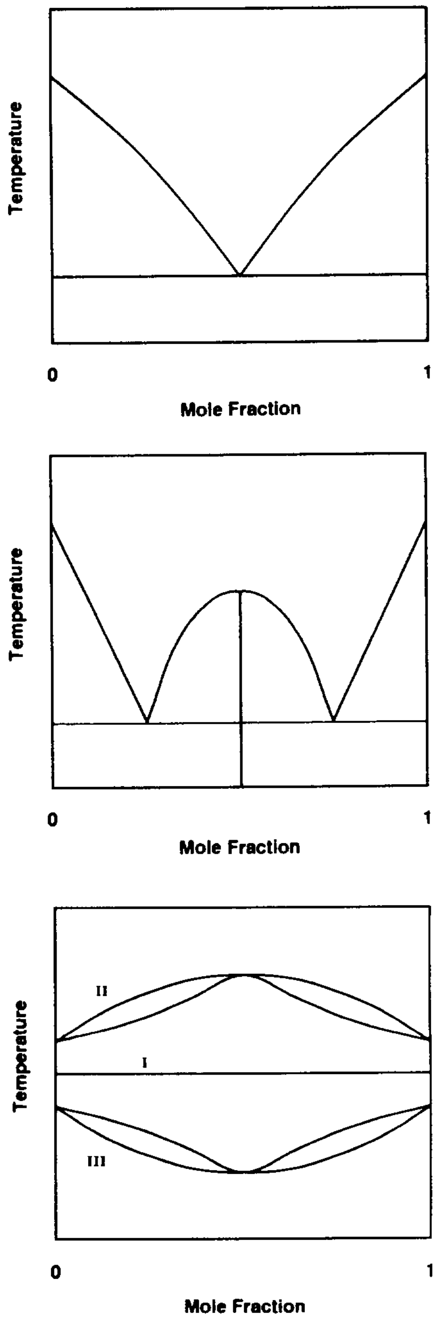

Fig. 6. Binary phase diagrams illustrating (a) conglomerates, (b) racemic compounds and (c) mixed crystals.

ture and entropy of fusion of the pure substances together with the excess function coefficients for the enthalpy and the entropy.

A general expression for the molar Gibbs energy G^{α} of a specified mixed state α of a binary system is

$$G^{\alpha}(T, x) = (1-x)G_1^{*,\alpha}(T) + xG_2^{*,\alpha}(T) + RT\ln(x) + G^{E,\alpha}(x, T) \tag{2}$$

where $LN(x) \equiv (1-x)\ln(1-x) + x\ln(x)$.

$G^{E,\alpha}$ is the molar excess Gibbs energy for state α, i.e. its deviation from ideal mixing behaviour. The symbol * stands for pure component properties. The excess Gibbs energy difference between the solid and the liquid state at the temperature of fusion can be described as

$$\Delta_{\mathrm{sol}}^{\mathrm{liq}} G^{E}(x) = \Delta_{\mathrm{sol}}^{\mathrm{liq}} H^{E}(x) - T_{\mathrm{fus}}(x)\Delta_{\mathrm{sol}}^{\mathrm{liq}} S^{E}(x) \tag{3}$$

In the calculation of the binary T_x phase diagram of the solid–liquid equilibrium of *d*- and *l*-carvone, the following assumptions were made (see also Ref. [8]): I. The liquid state is an ideal mixture. II. Heat capacity influences can be ignored. III. The excess enthalpy and the excess entropy are independent of temperature. IV. The excess functions can be described by: $\mathrm{exc} = cx(1-x)$.

The entropy of a pure substance can be determined from the measured temperature and enthalpy of melting as $\Delta_{\mathrm{sol}}^{\mathrm{liq}} S^* = \Delta_{\mathrm{sol}}^{\mathrm{liq}} H^*/T^*$. Since the components involved are enantiomers, they have equal temperature and entropy of fusion. From the DSC measurements, we obtained a temperature of fusion of 247.7 K and an entropy of fusion of $46.6\ \mathrm{J\,K^{-1}\,mol^{-1}}$.

The excess function coefficient for the enthalpy is determined using the measured temperature and enthalpy of fusion of the mixtures. From the fact that H_1^* and H_2^* are equal and in view of the assumptions I to IV, the enthalpy function is the following

$$\Delta_{\mathrm{sol}}^{\mathrm{liq}} H(x) = H^{\mathrm{liq}}(x) - H^{\mathrm{sol}}(x) = H^{*,\mathrm{liq}} - (H^{*,\mathrm{sol}} + H^{E,\mathrm{sol}}(x)) = \Delta_{\mathrm{sol}}^{\mathrm{liq}} H^* - hx(1-x) \tag{4}$$

The value of the excess function coefficient can easily be obtained from the experimental enthalpy values as described by Eq. (1): $\Delta_{\mathrm{sol}}^{\mathrm{liq}} H(x) = \{11541 - 10233(1-x)\}\ \mathrm{J\,mol^{-1}}$. Consequently, $h = 10233\ \mathrm{J\,mol^{-1}}$.

The excess function coefficient for the entropy can be determined using merely the temperature and enthalpy of fusion of the mixtures with compositions $x = 1$ and $x = 0.5$, as will be discussed below.

The intersection of the G^{sol} and G^{liq} surfaces is given by

$$\Delta_{\mathrm{sol}}^{\mathrm{liq}} G \equiv G^{\mathrm{liq}} - G^{\mathrm{sol}} = 0 \tag{5}$$

The equal-G curve [9] is the projection of this intersection on the Tx plane and has the general property of lying between the solidus and the liquidus. In the proposed phase diagram, the melting temperature of the equimolar mixture lies exactly on the equal-G curve. Consequently, $\Delta_{\mathrm{sol}}^{\mathrm{liq}} G_{(x=0.5)} = 0$. Therefore the entropy of melting at

$x=0.5$ can be described as

$$\Delta_{\mathrm{sol}}^{\mathrm{liq}}S_{(x=0.5)}=\Delta_{\mathrm{sol}}^{\mathrm{liq}}S^{*}-sx(1-x)=\frac{\Delta_{\mathrm{sol}}^{\mathrm{liq}}H_{(x=0.5)}}{T_{\mathrm{egc}(x=0.5)}}=\frac{\Delta_{\mathrm{sol}}^{\mathrm{liq}}H^{*}+hx(1-x)}{T_{\mathrm{egc}(x=0.5)}}, \tag{6}$$

resulting in the following equation for the excess function coefficient of the entropy

$$s=4\left(\Delta_{\mathrm{sol}}^{\mathrm{liq}}S^{*}-\frac{\Delta_{\mathrm{sol}}^{\mathrm{liq}}H^{*}+hx(1-x)}{T_{\mathrm{egc}(x=0.5)}}\right). \tag{7}$$

Summarising, the data entered in the Prophase program were: $T^{*}=247.7\,\mathrm{K}$; $\Delta S^{*}=46.6\,\mathrm{J\,mol^{-1}}$; $h=10233\,\mathrm{J\,mol^{-1}}$; $s=30.8\,\mathrm{J\,K^{-1}\,mol^{-1}}$.

Fig. 4 shows that the calculated values agree with the experimental data which demonstrates the thermodynamic consistency of the proposed phase diagram.

Another argument strengthening the conclusion that *d*- and *l*-carvone do form mixed crystals is the fact that the system behaves according to the characteristic properties generally observed when dealing with mixed crystals [8]. The quotient of the measured excess enthalpy and excess entropy is positive, namely $\Theta=\Delta_{\mathrm{sol}}^{\mathrm{liq}}H^{E}_{(x=0.5)}/\Delta_{\mathrm{sol}}^{\mathrm{liq}}S^{E}_{(x=0.5)}=2558.3/7.71=332\,\mathrm{K}$. This constant Θ represents a characteristic temperature for the given system which is above the melting range of the system [8].

In the case of mixed crystals, this characteristic temperature Θ is assumed to be related to the temperature of the equal-*G* curve at $x=0.5$ according to the following equation [8]

$$Q=\log\Theta/\log T_{\mathrm{egc}(x=0.5)}=1.10\pm0.05 \tag{7}$$

Carvone satisfies this rule since its Q value is 1.07. This confirms that the carvone system forms mixed crystals at all compositions.

5. Conclusions

A DSC curve of pure *l*-carvone shows a glass transition at 171 ± 1 K, followed by a large crystallisation peak, a small recrystallisation event, and finally the melting. The measured temperature and heat of fusion were $(247.7\pm0.5)\,\mathrm{K}$ and $(11.55\pm0.05)\,\mathrm{kJ\,mol^{-1}}$ respectively.

DSC measurements on mixtures of *d*- and *l*-carvone indicated that mixed crystals were formed. The solid–liquid phase diagram of carvone has a minimum. The data obtained using the computer program Prophase demonstrate the thermodynamic consistency of the phase diagram.

From the phase diagram and the change of the heat of fusion with composition, the change of the thermodynamic excess properties on melting has been calculated. The quotient of the excess enthalpy and excess entropy differences is found to be in line with the general rule observed for mixed crystals.

References

[1] J. Jacques, A. Collet and S.H. Wilen, Enantiomers, Racemates and Resolutions, Krieger Publishing Company, Florida, Reprint Ed., 1991.
[2] A.I. Kitaigorodskii, Organic Chemical Crystallography, Consultant Bureau, New York, 1961, p. 230.
[3] B. Chion, J. Lajzerowicz, D. Bordeaux, A. Collet and J. Jacques, J. Phys. Chem., 82(25) (1978) 2682.
[4] Y. Haget, J. Chim. Phys., 90 (1993) 313.
[5] G.W.H. Höhne, H.K. Cammenga, W. Eysel, E. Gmelin and W. Hemminger, Thermochim. Acta, 160 (1990) 1. For minor details, see G.W.H. Höhne, Proc. of the T.A.W.N. conference, Calibration of Heat-flux and Power Compensating DSC's, Utrecht, The Netherlands, June 1993.
[6] H.W. Bakhuis Roozeboom, Z. Phys. Chem., 28 (1899) 494.
[7] J.S. Van Duijneveldt, F.S.A. Baas and H.A.J. Oonk, Calphad, 13(2) (1989) 133.
[8] T. Calvet and H.A.J. Oonk, Calphad, 19(1) (1995) 49.
[9] H.A.J. Oonk, Phase Theory, Elsevier, Amsterdam, 1981.